

Numerical Determination of the Rate of Solidification in Centrifugal Casting

Iredia Erhunmwun , Anthony Osunde**

*University of Benin, Faculty of Engineering, Department of Production Engineering, Benin City, Nigeria

**Nigeria Prisons Staff School, behind medium security prisons, Oko, GRA, Benin City, Nigeria

*Corresponding Author : iredia.erhunmwun@uniben.edu
ORCID: 0000-0002-0497-8220

Received: 25.08.2020 Accepted:28.09.2020

Abstract- In centrifugal casting, it is not very easy to estimate experimentally the distribution of temperature as well as the solidification rate. Sequel to this, it is very difficult to have accurate data on the rate of solidification during centrifugal casting of different materials. Therefore, the need to determine numerically the solidification rate in centrifugal casting. The Finite Element Method was used to discretize and analyze the solidification thickness. The result obtained shows that at time $t=0$, the thickness was 0 cm since none of the liquid metal solidifies at the time of pouring the molten metal into the mold. At about 10sec from when the molten metal was poured into the mold, the solidified thickness of the cast was about 0.5 cm . At about 68 sec from when the molten metal was poured into the mold, molten metal was completely solidified. The total solidification time obtained in this research is 68 secs . This is still within the limit of foundry practice which is between 60 secs to 120 secs . This shows that the result obtained from this research is in agreement with the result obtained from finite difference method.

Keywords- Centrifugal casting, Solidification rate, Heat transfer, Finite Element Method, Solidification thickness

Özet- Santrifüj dökümde, sıcaklık dağılımını ve katılaşma oranını deneysel olarak tahmin etmek çok kolay değildir. Buna ek olarak, farklı malzemelerin santrifüj dökümü sırasında katılaşma hızına ilişkin doğru verilere sahip olmak çok zordur. Bu nedenle santrifüj dökümde katılaşma oranını sayısal olarak belirleme ihtiyacı vardır. Katılaşma kalınlığını ayırmak ve analiz etmek için Sonlu Elemanlar Yöntemi kullanıldı. Elde edilen sonuç, $t = 0$ anında, erimiş metalin kalıba dökülmesi sırasında sıvı metalin hiçbirinin katılaşmaması nedeniyle kalınlığın 0 cm olduğunu göstermektedir. Erimiş metalin kalıba dökülmesinden yaklaşık 10 saniye sonra, kalıbın katılaşmış kalınlığı yaklaşık 0.5 cm idi. Erimiş metal kalıba döküldükten yaklaşık 68 saniye sonra, erimiş metal tamamen katılaşmıştı. Bu araştırmada elde edilen toplam katılaşma süresi 68 saniyedir. Bu hala 60 saniye ile 120 saniye arasındaki dökümhane uygulaması sınırı içindedir. Bu durum, bu araştırmadan elde edilen sonucun sonlu farklar yönteminden elde edilen sonuçla uyumlu olduğunu göstermektedir.

Anahtar Kelimeler- Santrifüjlü döküm, Katılaşma hızı, Isı transferi, Sonlu Elemanlar Yöntemi, Katılaşma kalınlığı

1. Introduction

“Metal casting is a shape forming process whereby molten metal is poured into a prepared mold and allowed to solidify such that the shape of the solidified object is determined by the shape of the mold cavity” [1].

“In centrifugal casting, it is very difficult to determine the temperature distribution and solidification time by experimental techniques. As a result of this, accurate data on solidification time during centrifugal casting of different materials is scarce. Their estimation is a complex problem mainly because of the fact that the moving particles disturb the temperature equilibrium. Due to liquid and solid region in the casting during solidification, there is difference in thermo-

physical properties of different regions of casting during solidification” [2].

“The rate of solidification affects the microstructure, quality and mechanical properties of the castings. The analysis of heat transfer in centrifugal casting is very complex due to rapid solidification, rotating mold, opaque mold and high temperature. As the grain size is directly depending on the rate of solidification of the casting, based on grain size the rate of solidification of the centrifugal casting can be determined. Grain size has been measured for the gravity castings at different cooling rates and the rate of solidification of the centrifugal castings have been determined which are produced at different rotational speeds” [3].

“Investigation was carried out to determine the rate of solidification in permanent rectangular molds of varying thicknesses” [4]. “Solidification of metal casting is dependent on the rate of heat removal from the metal to the mold. This determines the solidification time, temperature, and microstructure. Therefore the understanding of the effect of mold thickness, time, and temperature can be a useful tool with which to improve process design and in turn control product quality. Also, a study was carried out to assess the effect of mold thickness on solidification time of a cylindrical cast to help improve casting process thereby producing high quality products” [5].

“The major defects in centrifugal casting are related to the solidification process, and it is not easy to take the temperature measurement of rotating body; therefore it is difficult to estimate the locations and magnitude of defects. Therefore, it is desirable to estimate solidification time through alternate means. Since the solidification process is related to the heat transfer of the casting-mold-ambient system, numerical simulation may be an effective method for evaluation. Mathematical modeling of the centrifugal casting process based on heat and mass transfer analysis can be a useful alternate methodology” [2]. Numerical solution of modeled equations using “Finite Element Method” has been attempted in this present study.

2. Mathematical formulation

The mathematical models used in centrifugal casting are based especially on heat transfer and solidification consideration of centrifugal casting. Figure 1 shows a schematic representation of the model of the centrifugal casting. “The heat is withdrawn from the liquid region of the casting to the metallic mold, and finally from mold to surrounding. Heat is also radiated away from the inner surface of the casting. As the solidification proceeds by conductive heat transfer through the molten metal in contact with metallic mold, the solid-liquid interface moves away from the metallic mold” [2].

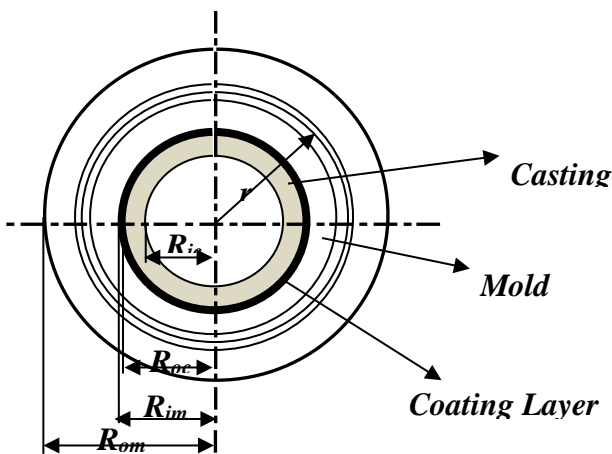


Fig. 1. Geometry of horizontal-axis centrifugal casting

The transient radially symmetric heat flow in the cylinder is governed by:

$$\frac{1}{r} \frac{\partial}{\partial r} \left(k_{\xi} r \frac{\partial T_{\xi}}{\partial r} \right) = C_{\xi} \rho_{\xi} \frac{\partial T_{\xi}}{\partial t} \tag{1}$$

Before pouring the liquid metal into the mold, the mold is preheated to a certain temperature to avoid thermal damage to the mold. Therefore, the initial temperature distributions in the casting, mold and shell regions are taken as:

$$\begin{aligned} T_c &= T_p \\ T_g &= T_m = T_M \end{aligned} \tag{2}$$

“As soon as the melt comes in contact with the mold wall, temperature of the metal-mold interface increases suddenly. Initial interface temperature is approximated by considering thermal energy conservation within the very thin layer of the metal and the mold in an adiabatic system” [6,7]. Since the heat flow rate from the metal to mold at the beginning is very rapid indeed, it can be stated that the liquid metal within this layer solidifies instantly.

“In order to find the metal-coating layer interface temperature at time $t=0$, the mold is assumed to be at a temperature T_M and the initial temperature of casting is assumed to be the temperature of the metal as it enters the mold cavity” [2].

The interface temperature can be written as

$$T_0 = \frac{\rho_g C_g T_M + \rho_L C_L T_p}{\rho_g C_g + \rho_L C_L} \tag{5}$$

The boundary conditions in different regions of the casting and mold are as follows:

1. At the inner surface of the casting, i.e., at $r = R_{ic}$,

$$k_{ic} \frac{\partial T_{ic}}{\partial r} = h_2 (T_{ci} - T_{\beta}) \tag{6}$$

$$\text{where } T_{\beta} = \frac{T_p + T_a}{2} \tag{7}$$

In the development of the weak form, we assumed a linear mesh and placed it over the domain. This was done by multiplying Equation (1) by the weighted function (w) and integrating the final equation over the domain. This results in the mathematical expression in Equation (8).

$$\frac{k_{\xi}}{C_{\xi} \rho_{\xi}} \int_{r_A}^{r_B} r \frac{\partial w}{\partial r} \frac{\partial T_{\xi}}{\partial r} dr + \int_{r_A}^{r_B} w \frac{\partial T_{\xi}}{\partial t} r dr - w Q_A - w Q_B = 0 \tag{8}$$

$$\text{where } -Q_A = \frac{w k_{\xi} r}{C_{\xi} \rho_{\xi}} \frac{\partial T_{\xi}}{\partial r} \Big|_{r_A} \text{ and } Q_B = \frac{w k_{\xi} r}{C_{\xi} \rho_{\xi}} \frac{\partial T_{\xi}}{\partial r} \Big|_{r_B} \tag{9}$$

Equation (8) is referred to as the weak form of the governing.

In the weak form, since the primary variable is simply the function itself, the Lagrange family of interpolation functions is admissible, therefore:

$$T_{\xi}(r, t) = \sum_{j=1}^n (T_{\xi})_j(t) \psi_j^e(r) \text{ and } w = \psi_i^e(r) \tag{10}$$

Substituting Equation (10) into Equation (8), we have:

$$[K_{ij}^e] \{T_{\xi}\}_j + [M_{ij}^e] \{\dot{T}_{\xi}\}_j = \{Q_i^e\} \tag{11}$$

where $K_{ij}^e = \frac{k_\xi}{C_\xi \rho_\xi} \int_{r_A}^{r_B} r \frac{\partial \psi_i^e}{\partial r} \frac{\partial \psi_j^e}{\partial r} dr$ (Conductivity Matrix) (12)

$$M_{ij}^e = \int_{r_A}^{r_B} r \psi_i^e \psi_j^e dr \text{ (Enthalpy Matrix)} \quad (13)$$

Next, we use the already developed finite element model of one-dimensional time-dependent problem to describe time approximation schemes and also convert the ordinary differential equation in time to algebraic equation. The α family of interpolation in which a weighted average of the time derivative of the dependent variable is approximated to two consecutive time steps by linear interpolation of the

$$[M_{ij}^e] \left[(1-\alpha) \left\{ \dot{T}_\xi \right\}_{j_s} + \alpha \left\{ \dot{T}_\xi \right\}_{j_{s+1}} \right] + [K_{ij}^e] \left[(1-\alpha) \left\{ T_\xi \right\}_{j_s} + \alpha \left\{ T_\xi \right\}_{j_{s+1}} \right] = (1-\alpha) \left\{ Q_i^e \right\}_s + \alpha \left\{ Q_i^e \right\}_{s+1} \quad (16)$$

The α family of interpolation for time consideration is given as:

$$(1-\alpha) \left\{ \dot{T}_\xi \right\}_{j_s} + \alpha \left\{ \dot{T}_\xi \right\}_{j_{s+1}} = \frac{\left\{ T_\xi \right\}_{j_{s+1}} - \left\{ T_\xi \right\}_{j_s}}{\Delta t_{s+1}} \quad (17)$$

$$\left[[M_{ij}^e] + \Delta t_{s+1} \alpha [K_{ij}^e] \right] \left\{ T_\xi \right\}_{j_{s+1}} = \left[[M_{ij}^e] - \Delta t_{s+1} (1-\alpha) [K_{ij}^e] \right] \left\{ T_\xi \right\}_{j_s} + \Delta t_{s+1} (1-\alpha) \left\{ Q_i^e \right\}_s + \Delta t_{s+1} \alpha \left\{ Q_i^e \right\}_{s+1} \quad (18)$$

Using the Backward Difference Scheme, where $\alpha = 1$, Equation 18 is reduced to Equation 19

$$\left\{ T_\xi \right\}_{j_{s+1}} = \left[[M_{ij}^e] + \Delta t_{s+1} [K_{ij}^e] \right]^{-1} \left[[M_{ij}^e] \left\{ T_\xi \right\}_{j_s} + \Delta t_{s+1} \left\{ Q_i^e \right\}_{s+1} \right] \quad (19)$$

2.1. Evaluating the elemental matrices

The one-dimensional Lagrange quadratic interpolation function for the equation becomes:

$$\psi_1(r) = \frac{1}{h_e^2} (h_e + r_A - r)(h_e - 2r + 2r_A) \quad (20)$$

$$\psi_2(r) = \frac{4}{h_e^2} (r - r_A)(h_e + r_A - r) \quad (21)$$

$$\psi_3(r) = \frac{-1}{h_e^2} (r - r_A)(h_e - 2r + 2r_A) \quad (22)$$

The Conductivity matrix can be easily derived by substituting the Lagrange interpolation functions in Equation (20) to (22) into Equation (12) respectively, we have:

$$[K^e] = \frac{k_\xi}{6h_e C_\xi \rho_\xi} \begin{bmatrix} 3h_e + 14r_A & -(4h_e + 16r_A) & h_e + 2r_A \\ -(4h_e + 16r_A) & 16h_e + 32r_A & -(12h_e + 16r_A) \\ h_e + 2r_A & -(12h_e + 16r_A) & 11h_e + 14r_A \end{bmatrix} \quad (23)$$

Also, the Enthalpy matrices can be easily derived by substituting the Lagrange interpolation functions in Equation (20) to (22) into Equation (13) accordingly, we have:

$$[M^e] = \frac{h_e}{60} \begin{bmatrix} h_e + 8r_A & 4r_A & -h_e - 2r_A \\ 4r_A & 16h_e + 32r_A & 4h_e + 4r_A \\ -h_e - 2r_A & 4h_e + 4r_A & 7h_e + 8r_A \end{bmatrix} \quad (24)$$

3. Result and discussion

values of the variables of the two steps is the most commonly used method for solving Equation (11). Therefore, we have:

For a given time step s and multiplying by $(1-\alpha)$, Equation 11 becomes

$$(1-\alpha) [K_{ij}^e] \left\{ T_\xi \right\}_{j_s} + (1-\alpha) [M_{ij}^e] \left\{ \dot{T}_\xi \right\}_{j_s} = (1-\alpha) \left\{ Q_i^e \right\}_s \quad (14)$$

For the next time step s+1 and multiplying by α , Equation 11 becomes

$$\alpha [K_{ij}^e] \left\{ T_\xi \right\}_{j_{s+1}} + \alpha [M_{ij}^e] \left\{ \dot{T}_\xi \right\}_{j_{s+1}} = \alpha \left\{ Q_i^e \right\}_{s+1} \quad (15)$$

Add Equation 14 and 15, we get

$$\text{Equation 17 can be used to reduce the ordinary differential equation in Equation 16 to algebraic equation. In other to do this, we substitute Equation 17 into Equation 16, we have:}$$

Equation 17 can be used to reduce the ordinary differential equation in Equation 16 to algebraic equation. In other to do this, we substitute Equation 17 into Equation 16, we have:

$$\text{Using the Backward Difference Scheme, where } \alpha = 1, \text{ Equation 18 is reduced to Equation 19}$$

$$\text{The following thermo physical properties, design and operating parameters has been used to analyse the developed model for both the casting and mold material. An alloy of 25% Chromium and 20% Nickel steel is used as the liquid metal with 0.4% Carbon steel as the mold material to determine the accuracy of the developed model with results available in literature. Different design and operating parameters, such as geometric constants for both the casting and the mold, the heat transfer coefficient at different regions of casting and the mold, and initial temperatures of mold and metal used in the analysis are as shown in Tables 1 and 2.}$$

Table 1. Thermo physical properties

Thermo Physical Properties	25%Cr-20%Ni Steel	0.4 % Carbon Steel	Coating Layer
K_d (cal/cmsec ⁰ C) at 0 ⁰ C	0.025	0.12	2x10 ⁻²
ρ (gr/cm ³)	7.3	7.8	5.7
C (cal/gm ⁰ C)	0.118	0.1	0.08
T_s (⁰ C)	1300	-	-
T_L (⁰ C)	1400	-	-
T_f (⁰ C)	1300	-	-
ΔH (cal/gr)	60	-	-

Table 2. Design and operating parameters

Outer diameter of steel mold, (cm)	31
------------------------------------	----

Outer diameter of casting, (cm)	13
Inner diameter of casting, (cm)	9
Damping coefficient between the mold-metal interface, β	0.83
Heat transfer coefficient at outer surface of steel mold (h_2) and at inner surface of casting (h_1), ($cal/cm^2sec^{\circ}C$)	0.00
Initial pouring temperature, $T_p(^{\circ}C)$	1500
Initial mold temperature, $T_m(^{\circ}C)$	250
Ambient temperature, $T_a(^{\circ}C)$	25
Emissivity at outer surface of mold, ϵ_M	0.4

4. Solidification Thickness Calculation

At this time, it is very pertinent to estimate the solidified thickness as time increases. It is evident from Figure 2 that as the time increases, the solidified thickness will also increase significantly. This is as a result of the fact that, as the time increases, more heat is being withdrawn from the liquid cast into the mold and finally into the atmosphere. From Figure 2, it is observed that at time $t=0$, the thickness was 0 cm since none of the liquid metal solidifies at the time of pouring the molten metal into the mold. Also, at about 10 sec from when the molten metal was poured into the mold, the solidified thickness of the cast was about 0.5 cm . Finally, at about 68 sec from when the molten metal was poured into the mold, the solidified thickness of the cast was about 2 cm . This means that at this time all the liquid cast has been completely solidified.

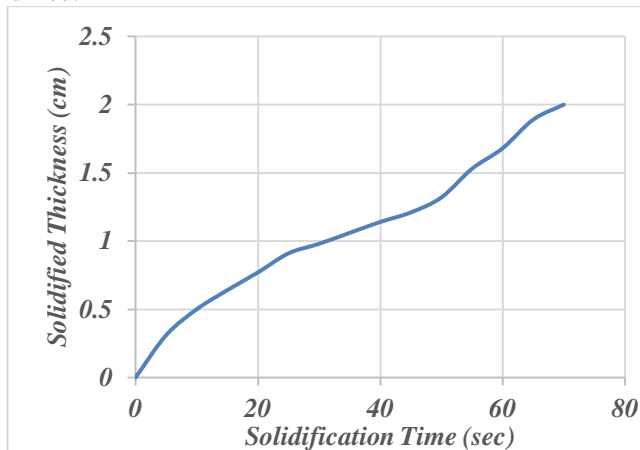


Fig 2. A graph of Solidified Thickness against Solidification Time

5. Comparison with Results Available in Literature

It is evident from the graphs for temperature profiles that solidification starts from the molten metal in contact with the inner mold wall and proceeds right across the inner section until last solidifying metal freezes at inner bore, therefore the chances of shrinkage cavity is more at inner bore as compare to other region of solidifying metal. The total solidification time obtained by Fixed domain method has a maximum value of 70 secs , while by Variable domain method has a maximum value of 100 secs as mentioned in the work of Kamlesh [2]. The solidification time obtained in this research has a

maximum value of 68 secs . This is still within the limit of foundry practice which is between 1 min to 2 mins [6].

To validate the result from this research, we compare our result with the result obtained by Kamlesh [2] where the author used the Finite Difference Method. “The disadvantage of using the Finite Difference method is that the usual procedure for deriving finite-difference equations consists of approximating the derivatives in the differential equation via a truncated Taylor series. The method includes the assumption that the variation of the dependent variable is somewhat like a polynomial in the independent variable, so that the higher derivatives are unimportant. This assumption, however, leads to an undesirable formulation when exponential variations are encountered. The Taylor-series formulation is relatively straightforward but allows less flexibility and provides little insight into the physical meanings of the terms” [8].

6. Conclusion

In this study, the finite element method has been used to determine the solidification rate in horizontal centrifugal casting with consideration to the solidification time. The results obtained from the FEM were compared with the results obtained from the finite difference method and it was observed that both results agrees. The result obtained shows that the finite element method is an efficient and accurate method.

References

- [1] A.O.A. Ibadode,(2014) Introduction to Manufacturing Technology, TETFUND Edition, Ambik publishers, Benin City, Nigeria
- [2] Kamlesh,(2001) Ph.D. Thesis, BVM Engineering College, Gujarat, India, p. 35.
- [3] Madhusudhan, S. Narendranath, G.C. Mohan Kumar, (2012)“Experimental Study on Cooling Rate of Centrifugal Casting Based on Grain Size” International Journal of Scientific & Engineering Research, Vol. 3, No. 1, pp. 1- 3.
- [4] K.C. Bala, R.H. Khan, M.S. Abolarin, O.K. Abubakre, “Investigation on the rate of solidification and mold heating in the casting of commercially pure aluminium in permanent molds of varying thickness”, IOSR Journal of Mechanical and Civil Engineering, 6(1), p. 33-37.
- [5] K.C. Bala, R.H. Khan, (2014) “Rate of of solidification aluminium casting in varying wall thickness of cylindrical metallic molds”. Leonardo Journal of Sciences, vol. 25, pp. 19-30.
- [6] Y. Ebisu.(1977)“Computer simulation on Macrostructure in Centrifugal Castings”, AFS Transactions, pp 643-655,
- [7] R.D. Phelke, M.J. Kirt, R.E. Marrone, D.J. Cook, (1974)“Numerical Simulation of Casting Solidification”, AFS Illinois, pp. 1-7.
- [8] E. Panda, D. Mazumdar, S.P. Mehrotra, (2006) “Mathematical modeling of particle segregation during centrifugal casting of metal matrix composites”, Metall. Mater. Trans. A, vol. 37A, pp. 1675–1687.